

## Moment of inertia, backbending, and molecular bifurcation

Vivian Tyng and Michael E. Kellman

*Institute of Theoretical Science, Department of Chemistry, University of Oregon, Eugene, Oregon 97403*

(Received 8 June 2007; accepted 3 July 2007; published online 27 July 2007)

We predict an anomaly in highly excited bending spectra of acetylene with high vibrational angular momentum. We interpret this in terms of a vibrational shape effect with moment of inertia backbending, induced by a sequence of bifurcations with a transition from “local” to “orthogonal” modes. © 2007 American Institute of Physics. [DOI: 10.1063/1.2766936]

Around 25 years ago, it became clear that profound changes in the vibrational dynamics of molecules occur when nonlinearities can no longer be treated as perturbative effects, and the standard picture of anharmonic normal modes breaks down. This perspective has since been developed in many studies. Numerous references can be found in a recent study of acetylene bend spectra<sup>1</sup> and a recent review.<sup>2</sup>

We have emphasized particularly the role of bifurcations in the “birth of new modes from the low energy normal modes.” Spectral phenomena associated with bifurcations have been predicted and observed. While bifurcation effects in purely vibrational dynamics and spectra are starting to be well understood, the interplay of bifurcations and angular momentum remains mostly a mystery. There has been work on the effects of angular momentum on vibrational bifurcations.<sup>3</sup> Here we will concentrate on the converse: effects of vibrational bifurcations on the angular momentum spectrum. We know of one other investigation<sup>4</sup> in this vein and will describe its relation to the work here in due course.

In this paper we want to focus on bifurcation effects in spectra of as elementary a system as possible. General angular momentum phenomena will involve the full rotation-vibration problem. We therefore deliberately seek to minimize rotation-vibration interactions such as Coriolis couplings. To this end, we consider pure vibrational angular momentum  $J=\ell$  excitations of a linear molecule in highly excited bending states. We choose acetylene because it has a highly refined effective spectroscopic fitting Hamiltonian<sup>5</sup> which can be extrapolated to make predictions about high angular momentum spectra. As desired, the  $J=\ell$  pure vibrational angular momentum states are minimally affected by rotation-vibration interactions.<sup>6</sup> From the effective fitting Hamiltonian, we predict clearly anomalous spectral behavior. To understand this, we investigate a “moment of inertia backbending” effect as the molecule undergoes a sequence of bifurcations. Essentially, the molecule undergoes a change in vibrational “shape” due to the bifurcations while retaining its linear equilibrium symmetry.

Now we identify the spectral series of interest and present numerical evidence for anomalous behavior. In  $C_2H_2$  it turns out empirically<sup>5,7</sup> that to a good approximation there are pure bending excitations, decoupled from the stretch modes, with conserved bend quantum number  $N_b$ . We will

consider  $J=\ell$  angular momentum excitations  $[N_b, \ell] = [N_b, 0], [N_b, 1] \cdots [N_b, \ell_{\max}]$ , with  $\ell_{\max}=N_b+2$  in each  $N_b$  series. The states considered are the ones of *lowest energy* for each polyad  $[N_b, \ell]$ . Classically, these excitations possess fully stable character;<sup>6</sup> as such, the  $\ell=0$  members correspond to the reaction path in the acetylene-vinylidene isomerization.<sup>8</sup>

An anomaly in these spectral series is visible as a very slight undulation in a plot of energy versus  $\ell$  for a given series  $[N_b, \ell]$ . We do not show this here; instead we analyze it by plotting energy differences between succeeding levels in the series. This corresponds semiclassically to a plot of  $\omega = \partial H / \partial \ell$  vs  $\ell$ . This is shown for the series  $N_b=18-29$  in Fig. 1. Sharply differentiated sectors are evident in these series.

To interpret this anomalous behavior, we will consider a moment of inertia backbending effect and its physical explanation in terms of bifurcations. Backbending involves a series of angular momentum excitations. A familiar instance is seen when an ice skater induces “spin up” or “spin down” by pulling the arms in or out. In classical mechanics, the system can be viewed as a rotating quasirigid body:

$$E = \frac{I\omega^2}{2} = \frac{J^2}{2I}, \quad (1)$$

with effective angular frequency  $\omega$  and moment of inertia  $I$  determined as<sup>9</sup>

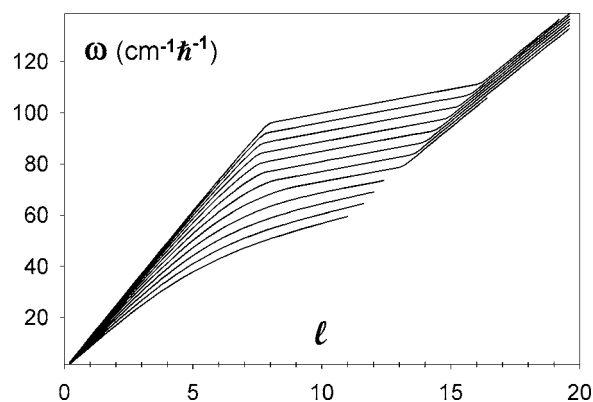


FIG. 1. Predicted semiclassical  $(\ell, \omega)$  from energy level differences of Eqs. (2) and (3) for  $N_b=18, 19, \dots, 29$ .

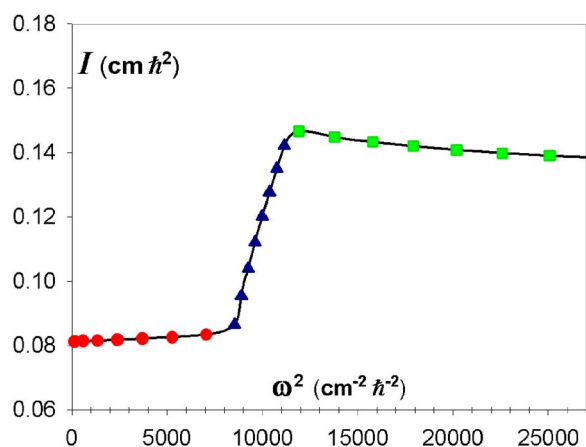


FIG. 2. (Color online) Predicted  $(\omega^2, I)$  for polyads  $[N_b, \ell] = [28, 1], [28, 2], \dots, [28, 22]$  of the  $N_b=28$  series. The sectors are L [circles (red)], OGC [triangles (blue)], and O [squares (green)].

$$\omega = \frac{J}{I} = \frac{dE}{dJ} \approx \frac{E(J + \Delta J) - E(J - \Delta J)}{2\Delta J}, \quad (2)$$

$$I = \frac{dJ^2}{2dE} \approx \frac{2J\Delta J}{E(J + \Delta J) - E(J - \Delta J)}, \quad (3)$$

with  $J$  here taken to be the rotational angular momentum in units of  $\hbar$ . For a rigid body,  $I$  is of course a constant. For a semirigid body,  $I$  normally increases steadily with  $\omega$  (and  $\omega^2$ ) as a result of the centrifugal force. However, in moment of inertia backbending, the curve of  $(\omega^2, I)$  exhibits an  $S$ -shaped segment: the slope suddenly becomes negative at some rotational frequency before resuming the positive slope. There may be incomplete backbending, sometimes called “upbending.” Both backbending and upbending have been observed in nuclei<sup>10</sup> and predicted in stars<sup>11</sup> and electronic curve crossings in diatomic molecules.<sup>9</sup> However, the situation in those cases differs in the fundamental respect that the backbending is concerned with rotational angular momentum perpendicular to the symmetry axis, while here the angular momentum is parallel to the symmetry axis with  $J=\ell$ .

Figure 2 shows the predicted  $(\omega^2, I)$  plot for the series with  $N_b=28$ , calculated by the finite differences on the right hand side in Eqs. (2) and (3). Moment of inertia upbending is evident. There are clearly three sectors in the figure, labeled L, OGC, and O for reasons that will become apparent. Figure 3 shows the  $(\omega^2, I)$  plot for the series with  $N_b=8-38$  collected together. Each series terminates at the maximal value  $\ell=N_b+2$  allowed for the given  $N_b$ . It is evident that all of the series show upbending, with an abrupt onset of the upper flattened sector at  $N_b=22$  and a sharpening of the lower corner of the  $S$  curve with increasing  $N_b$ .

To account for the upbending, we consider the bifurcation behavior of acetylene. A bifurcation is accompanied by a change of molecular shape (in a special dynamical sense to be made explicit later; we are not speaking of a change in equilibrium geometry of the molecule). At low quantum numbers, the modes are the familiar normal modes. Due to anharmonicity and couplings, at higher quantum numbers, the normal modes bifurcate and new modes are formed; these, in turn, can undergo further bifurcations.

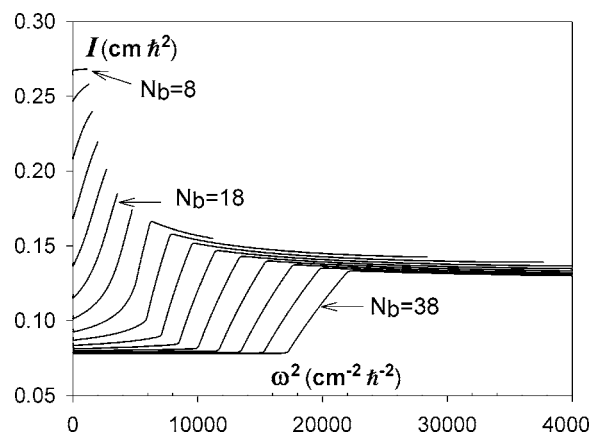


FIG. 3. Predicted  $(\omega^2, I)$  for  $[N_b, \ell]$  series with  $N_b=8, 10, \dots, 38$ .

The bifurcation analysis works as follows. A classical version of the quantum matrix fitting Hamiltonian<sup>12</sup> is obtained via the Heisenberg correspondence.<sup>13</sup> The effective Hamiltonian for acetylene<sup>5</sup> has  $N_b$  and  $\ell$  as conserved quantities. We obtain a reduced classical Hamiltonian by projecting out these conserved actions and their conjugate angles. The bifurcation analysis is then performed by finding the critical points of the reduced Hamiltonian.<sup>1,7,14-16</sup> The critical points for a given  $[N_b, \ell]$  are found by solving analytic algebraic equations; there is no need to integrate Hamilton’s equations. Along a sequence of critical points with fixed  $N_b$  and varying  $\ell$ , the quantities

$$\omega = \partial H / \partial \ell, \quad (4)$$

$$2I = \partial \ell^2 / \partial H \quad (5)$$

are calculated semiclassically according to Eqs. (2) and (3) to give the curves in Figs. 2 and 3.

When  $\ell=0$ , there are four bifurcations in which the *trans* bend normal mode spawns new modes called local L, orthogonal O, and precessional P, and the *cis* bend normal mode bifurcates to give a counter-rotator CR mode. The dramatically different nature of these new modes from the normal modes is seen clearly in still figures<sup>1,2</sup> and web-based animations.<sup>17</sup>

When  $\ell > 0$ , bifurcations again give the four new modes L, O, P, and CR, and in addition,<sup>6</sup> for some  $[N_b, \ell]$  a new family called “off great circle” OGC. A still figure depiction of the O mode will be considered below in Fig. 4. At fixed  $N_b$  sufficiently large, there is a bifurcation sequence  $L \rightarrow \text{OGC} \rightarrow O$  in the direction of increasing  $\ell$ , in which the L mode (itself born in a bifurcation of the *trans* normal mode) bifurcates to give an OGC mode, which then bifurcates to give an O mode. [Following the states of the bifurcation sequence is the same as using the energy level excitation sequences of Eqs. (2) and (3).]

Figures 2 and 3 represent an interpretation of the predicted vibrational series as rotational excitation of a system with  $J=\ell$  and moment of inertia  $I$  along the molecular axis and associated rotation frequency  $\omega$ , as given by Eqs. (2) and (3). The crucial observation is that the three distinct regions of the moment of inertia curves correspond to the three sectors in the bifurcation sequence  $L \rightarrow \text{OGC} \rightarrow O$ . However,

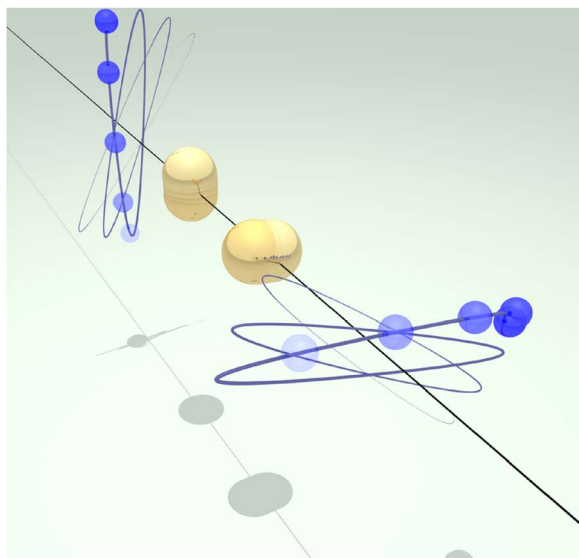


FIG. 4. (Color online) Time-lapse figure of the precessing orthogonal mode O for  $N_b=20$ ,  $\ell=4$ , adapted from Ref. 2.

acetylene is a linear molecule, conventionally thought of in its equilibrium configuration as having zero moment of inertia along the figure axis. Then what meaning is to be attached to the moment of inertia  $I$  and the rotation frequency  $\omega$  in Figs. 2 and 3?

The moment of inertia can be understood in terms of breaking of the  $D_{\infty h}$  molecular symmetry, which of course occurs with vibrational angular momentum excitation and associated centrifugal effects. The rapid vibrational motion with high  $N_b$  and  $J=\ell=0$  creates a vibrational shape. The shape then has slower angular momentum excitations with  $J=\ell \neq 0$  along the symmetry axis. A *variable* moment of inertia comes about because of the changing shape along the curves in Figs. 2 and 3 in the sequence L  $\rightarrow$  OGC  $\rightarrow$  O.

A visual image of the molecular shape and its collective rotation is useful. Figure 4 shows a time-lapse picture of the orthogonal mode, the O sector in Figs. 2 and 3. At each end, the H atom of the molecule moves in a rapid trajectory in a near ellipse. However, instead of closing on itself, the ellipse precesses. The two ends of the molecule have the elliptical shapes oriented at right angles to each other, with a definite fixed angle  $\approx \pi/2$  between the orbits, and the whole system slowly precessing in phase. Viewed along the figure axis, the molecule has the rotational symmetry about the  $D_{\infty h}$  axis “spontaneously broken” into a cross shape. It is this symmetry breaking that enables the whole vibrational shape to rotate collectively about the molecular axis (precession of the ellipses in phase), thereby restoring the rotational symmetry.

This is readily given a clear mathematical expression. The cross shape is determined by the fixed angle relationship of the precessing ellipses, which comes from the critical point analysis. The frequency of the rapid motion that creates the shape is the frequency  $\Omega_b$  of oscillation of the elliptical orbits. The slower rotational frequency  $\omega$  of the shape is the frequency of precession of the orbits. These frequencies are given, respectively, by the partial derivatives of the Hamiltonian with respect to the actions  $N_b$  and  $\ell$ :

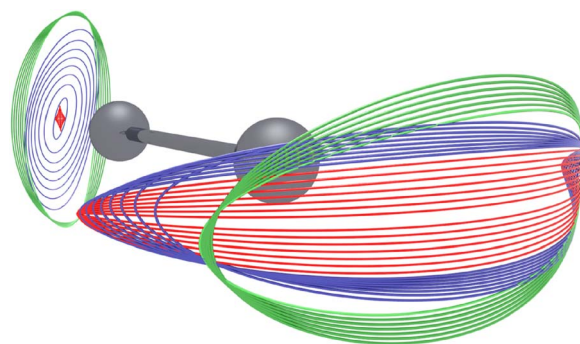


FIG. 5. (Color online) Superposition of ellipses of trajectories from members  $[N_b, \ell]=[28,1],[28,2], \dots, [28,22]$  of the  $N_b=28$  series. The inner (red), middle (blue), and outer (green) groups of trajectories belong, respectively, to the sectors L, OGC, and O of Fig. 2. Overall precession around the C-C axis (as in Fig. 4) is eliminated in order to focus on the change in the elliptic shapes.

$$\Omega_b = \partial H / \partial N_b, \quad \Omega_\ell = \omega = \partial H / \partial \ell. \quad (6)$$

A physical understanding can now be realized of the S-shaped behavior of the moment of inertia curves. In Fig. 5 for the series  $N_b=28$ , for each  $\ell$  value in the series, we plot each classical trajectory (without precession) at both ends of the molecule. As clearly seen in the resulting collage of trajectories, there are three sectors, corresponding to L, OGC, and O. This shows how a characteristic vibrational shape is maintained for each type of critical point and then changes sharply at the bifurcation points in the L  $\rightarrow$  OGC  $\rightarrow$  O sequence. It is noteworthy that the upbending part of the moment of inertia curve is associated with the OGC segment of the bifurcation sequence. In phase space, the OGC is a transitional sector that bridges L and O, which are locked at their own fixed angles in the phase space.

It is worthwhile to relate this picture to the usual treatment of a linear molecule with doubly degenerate vibrations, for example, by Herzberg.<sup>18</sup> He treats a vibrating linear molecule as a symmetric top with energy contribution

$$BJ(J+1) + A\ell^2 \quad (7)$$

from the angular momentum. This is somewhat different from Fig. 5 in which the vibrational shape is not necessarily that of a prolate symmetric top, as is readily seen in the local mode sector in the figure. In relation to the treatment of Ref. 18, our conception is of a fast vibrational motion that creates the shape, and a slower but still *relatively fast* precessional motion (“rotation” parallel to the figure axis) that restores the  $D_{\infty h}$  prolate symmetric top symmetry, i.e., both frequencies  $\Omega_b$  and  $\Omega_\ell$  are fast compared to the “rotational” frequency about an axis perpendicular to the molecule. With rotation-vibration interaction, the symmetric top energy level pattern is broken by  $\ell$  doubling.<sup>18</sup> As discussed above, in the system here with pure vibrational angular momentum excitations  $J=\ell$ , rotation-vibration effects are minimized (and absent in the classical limit<sup>6</sup>). The effective Hamiltonian of Ref. 5 has no Coriolis terms, and our predicted spectra lack the very slight expected  $\ell$  doubling; the spectrum is that of a symmetric top. The novelty of the situation described here resides entirely in the effects of the bifurcations on the spectrum and associated frequency and moment of inertia plots.

We mentioned at the beginning the work of Ishikawa *et al.*<sup>4</sup> which discusses the observed effects of a saddle-node bifurcation on the moments of inertia in HCP. In that kind of bifurcation, a novel mode with its own moment of inertia erupts “out of nowhere” in phase space. In the situation discussed in the present work, the bifurcation is of the existing L mode in a bifurcation sequence, with a gradual transition in the moment inertia. The difference between the situations in Ref. 4 and the backbending effect treated here is akin to that between first and second order phase transitions.

We have used the effective fitting Hamiltonian of acetylene to predict a sequence of bifurcations that produces anomalous spectra with a moment of inertia backbending effect. An experimental test would be more interesting.

This work was supported by the U.S. Department of Energy Basic Energy Sciences program under Contract No. DE-FG02-05ER15634.

<sup>1</sup>V. Tyng and M. E. Kellman, *J. Phys. Chem. B* **110**, 18859 (2006).

<sup>2</sup>M. E. Kellman and V. Tyng, *Acc. Chem. Res.* **40**, 243 (2007).

<sup>3</sup>Ch. van Hecke, D. A. Sadovskii, B. I. Zhilinskii, and V. Boudon, *Eur.*

*Phys. J. D* **17**, 13 (2001).

<sup>4</sup>H. Ishikawa, R. W. Field, S. C. Farantos, M. Joyeux, J. Koput, C. Beck, and R. Schinke, *Annu. Rev. Phys. Chem.* **50**, 443 (1999).

<sup>5</sup>M. P. Jacobson, J. P. O'Brien, R. J. Silbey, and R. W. Field, *J. Chem. Phys.* **109**, 121 (1998).

<sup>6</sup>V. Tyng and M. E. Kellman, report (unpublished).

<sup>7</sup>J. P. Rose and M. E. Kellman, *J. Chem. Phys.* **105**, 10743 (1996).

<sup>8</sup>D. Xu, H. Guo, S. Zou, and J. M. Bowman, *Chem. Phys. Lett.* **377**, 582 (2003).

<sup>9</sup>L. P. Marinova, P. P. Raychev, and J. Maruani, *Mol. Phys.* **82**, 1115 (1994).

<sup>10</sup>K. L. G. Heyde, *Basic Ideas and Concepts in Nuclear Physics*, 3rd ed. (IOP, Bristol, 2004).

<sup>11</sup>N. K. Glendenning, S. Pei, and F. Weber, *Phys. Rev. Lett.* **79**, 1603 (1997).

<sup>12</sup>M. E. Kellman, *Annu. Rev. Phys. Chem.* **46**, 395 (1995).

<sup>13</sup>M. S. Child, *Semiclassical Mechanics with Molecular Applications* (Clarendon, Oxford, 1991).

<sup>14</sup>L. Xiao and M. E. Kellman, *J. Chem. Phys.* **93**, 5805 (1990).

<sup>15</sup>Z.-M. Lu and M. E. Kellman, *J. Chem. Phys.* **107**, 1 (1997).

<sup>16</sup>S. Keshavamurthy and G. S. Ezra, *J. Chem. Phys.* **107**, 156 (1997).

<sup>17</sup><http://uoregon.edu/~meklab/>; <http://pubs.acs.org/subscribe/journals/jpcbfk/asap/objects/jp057357f/index.html>

<sup>18</sup>G. Herzberg, *Molecular Spectra and Molecular Structure III: Electronic Spectra and Electronic Structure of Polyatomic Molecules* (Van Nostrand Reinhold, New York, 1966), pp. 69–70.